

Improved final doublet designs for the ILC small crossing angle scheme

R. Appleby

*The Cockcroft Institute and the University of Manchester
Oxford Road, Manchester, M13 9PL, U.K.
E-mail: r.b.appleby@dl.ac.uk*

P. Bambade

*Laboratoire de l'Accélérateur Linéaire, CNRS/IN2P3 and Université Paris Sud 11
Bâtiment 200, B.P. 34, F-91898 Orsay, Cedex, France*

ABSTRACT: The International Linear Collider (ILC) baseline layout consists of two interaction regions, both with a 14 mrad beam crossing angle. The main alternative layout uses a small beam crossing angle of 2 mrad, and is preferred by the physics and detector communities. It is known that the outgoing beam losses in the final doublet and subsequent extraction line are larger in the 2 mrad than in the 14 mrad layout. In this work, we exploit NbTi and Nb₃Sn superconducting magnet technologies to redesign and optimise the final doublet region of the 2 mrad scheme, with the aim of providing satisfactory outgoing disrupted beam power losses in this region. We present three new final doublet layouts, specifically optimised for the 500 GeV and the 1 TeV machines.

KEYWORDS: Accelerator modelling and simulations (multi-particle dynamics; single-particle dynamics); Simulation methods and programs.

Contents

1. Introduction	1
2. Magnet parameters	2
2.1 Current baseline design	2
2.2 Maximum pole tip field for NbTi	3
2.3 Expected maximum pole tip field for Nb ₃ Sn	3
2.4 Outline of doublet designs	3
2.5 Assumed power deposition tolerances	3
3. Final doublet optimisation	4
4. Particle losses in the optimised final doublet	6
4.1 Results for E=500 GeV	7
4.2 Results for E=1 TeV	8
5. Conclusions	10

1. Introduction

The baseline configuration of the International Linear Collider (ILC) [1] consists of two interaction regions (IRs) and two detectors, with both IRs having a 14 mrad beam crossing angle. The 14 mrad crossing angle layout is derived from the large crossing angle design of the Next Linear Collider [2]. Its optical properties are well understood, and the extraction line successfully transports the disrupted beam to the dump, for a wide range of proposed beam parameter sets [3]. However an alternative crossing angle layout, which uses a small beam crossing angle, has been developed over the last few years. This 2 mrad crossing angle layout is preferred by the physics and detector communities, and offers advantages over the 14 mrad baseline layout. There is an ongoing effort to solve the technical challenges of this scheme, which mainly result from transporting the outgoing disrupted beam off-axis in the final doublet. The first complete optics was presented at Snowmass 2005 [4] and was developed for 1 TeV using NbTi superconducting final doublet magnets and included downstream energy and polarimetry measurement chicanes.

The current ILC parameter space is documented in [5] and the key parameters are listed in table 1. These consist of sets of representative beam parameters, designed to assure flexibility in case of unexpected practical limitations in achieving some of the machine goals. The most challenging of these sets is known as the High Luminosity set, which aims to maximise the instantaneous luminosity by more strongly focusing the beams at the interaction point (IP), thereby significantly

Set	Energy [GeV]	N_b	I_{av} [A]	δ_B	\mathcal{L} [$\text{m}^{-2} \text{s}^{-1}$]
Nominal	500	2820	0.0104	0.022	2.03E38
Low Power	500	1330	0.0069	0.057	2.05E38
High Lum.	500	2820	0.0104	0.070	4.92E38
Nominal	1000	2820	0.0104	0.050	2.82E38
Low Power	1000	1330	0.0069	0.134	2.92E38
High Lum.	1000	2820	0.0104	0.178	7.88E38

Table 1. Key parameters of the beam parameter sets used in this work.

enhancing disruption effects. A necessary criterion for the performance of the extraction line design is its ability to accommodate the broadest possible range of beam parameters. The 14 mrad scheme is successful for the majority of parameter sets, but the current 2 mrad design shows unacceptable beam power loss, both in the final doublet and in the extraction line, for some of the beam parameters considered.

In this work, we exploit the limits of current magnet technology as well as technology still under development to optimise the 2 mrad final doublet layout. We present three new final doublet designs, one optimised for the baseline energy of 500 GeV and two for the upgrade energy of 1 TeV. We optimise the magnet parameters with respect to power deposition from charged beam and radiative Bhabha particle losses, with the goal of accommodating all ILC beam parameter sets. We find that this is possible by using NbTi technology for the 500 GeV machine, and by using new Nb₃Sn technology for the 1 TeV upgrade. However, an increase in pole tip field, somewhat beyond the currently planned limits for Nb₃Sn technology, would be required to achieve power losses small enough to avoid quenching of the final doublet magnets for the case of the Low Power and High Luminosity beam parameters at 1 TeV. We include a full set of magnet and optical parameters for evaluation by magnet designers.

In section 2 we discuss the available magnet technologies and the constraints we place on magnet parameters. We describe our final doublet optimisation procedure in section 3 and present the resulting magnet parameters for each case. The beam transport and resulting losses with our new doublets are presented in section 4, and we draw our conclusions in section 5. We find that the proposed new final doublet layouts have considerably better beam transport properties than the current ones.

2. Magnet parameters

2.1 Current baseline design

The final doublet in the 2 mrad scheme is based a superconductive large bore QD0 magnet and on a normal conducting smaller aperture QF1 magnet. The two nearby sextupoles for local chromaticity correction, SD0 and SF1, are also superconductive large bore magnets. Note we refer to the 2 mrad scheme layout developed at Snowmass 2005 and documented in [4] as the 2 mrad baseline design. In this design, the choice of superconductive technology for QD0 is NbTi and the maximum pole tip field which is assumed to be achievable is 5.6 T. In this work we always take the distance from

the final magnet to the interaction point, l^* , to be 4.5 m and the QD0-QF1 distance to be 9 m. The outgoing beam passes through the coil pocket of QF1, where the field is modelled by a standard multipole expansion. The outer coil radius, which is available for beam passage, is 115 mm. The doublet was optimised for the TeV machine, and the 500 GeV layout was obtained by scaling down the fields.

2.2 Maximum pole tip field for NbTi

For the NbTi magnets [6] considered in this work, we assume a maximum pole tip field of 6.28 T. This is around the maximum field that current coil designs can produce, and includes the field-reducing effects of the external solenoid and a safety margin. This corresponds to a gradient of 180 T m^{-1} in a magnet of radial aperture 35 mm. The sextupoles are required to be large bore superconducting magnets, to allow the transport of the outgoing beam. We follow the technology choice of the current design, and adopt a maximum field of 4.04T in SD0 and SF1 (with radial apertures of 88 mm and 112 mm, respectively).¹

2.3 Expected maximum pole tip field for Nb₃Sn

We also propose to use Nb₃Sn-based technology [6] for QD0 at 1 TeV. The higher gradient permitted by this magnet will improve the beam transport properties of the doublet, by allowing a more compact design. These magnets have yet to be proven, but in the timescales of the ILC TeV upgrade, should hopefully be readily available. Of course, such an upgrade would require replacing the final doublet, but this is rather minor on the scale of the 1 TeV energy upgrade. Furthermore the geometry of the extraction line would need to be maintained. The maximum pole tip field which we assume will be achievable with Nb₃Sn is 8.8T (taking into account the presence of a solenoid background field). This corresponds to a 250 T m^{-1} gradient for a 35 mm radial aperture.

2.4 Outline of doublet designs

In this work, we propose three new doublet layouts. We shall optimise the layout for the 500 GeV machine, using NbTi for QD0 at a maximum pole tip field of 6.28 T. The beam transport properties of such a layout will be considerably better than the scaled down version of the 1 TeV existing scheme, because the magnet length can be reduced. The sextupoles shall be optimised versions of the current sextupoles. We shall then calculate the layouts for the TeV machine, firstly using NbTi for QD0 as the design for 500 GeV, and secondly with Nb₃Sn. The resulting doublets are intended to replace the baseline design.

The current scheme magnets are summarised in table 2. In table 3 we describe our proposed magnet technology limits for this work.

2.5 Assumed power deposition tolerances

Superconducting magnets will quench if too much beam power is deposited in them, and both integrated power and localised power density tolerances have been specified by the CERN group for the LHC quadrupoles used in this work. The maximum integrated power which can be tolerated

¹The maximum field in a sextupole probably has some dependence on its aperture. This point should be checked with experts, to assess the feasibility of our proposed magnets.

Magnet	Length [m]	Strength	radial aperture [mm]	gradient [T m ⁻¹]	B ^{PT} [T]
QD0	2.5	-0.0958 m ⁻¹	35	159.4	5.58
SD0	3.8	0.6254 m ⁻²	88	-	4.04
QF1	2.0	0.0407 m ⁻¹	10	67.8	0.68
SF1	3.8	-0.2039 m ⁻²	112	-	2.13

Table 2. Quadrupole and sextupole parameters at $\sqrt{s}=1$ TeV for the current baseline design.

Magnet	Type	Maximum field [T]
QD0 (NbTi)	SC	6.28
QD0 (Nb ₃ Sn)	SC	8.75
SD0	SC	4.04 (r=88mm)
QF1	NC	1.02
SF1	SC	2.13 (r=112mm)

Table 3. The limiting parameters of the final doublet magnets. Note that these maximum fields include the reductions expected from the solenoid background field at the location of the magnets.

per unit length is in the range 5-10 W m⁻¹ [6]. However, for a few specific magnets like those in the final doublet, this tolerance can presumably be relaxed if more cryogenic power can be used. The highest localised power density which can be accepted is 0.5 mW g⁻¹ [6]. This tolerance is important to consider in this work because the outgoing beam is transported off-axis through several of the final doublet magnets, and so particles at the lower end of the energy distribution can get over-focused onto the edge of the magnet aperture on one side. Since these particles are essentially concentrated in a plane (except for their vertical angular spread), the local power density can become high. We rely on detailed computations performed at RHUL with the GEANT-4 based BDSIM simulation [7]. These calculations have shown that for about 1 W incident beam power on the edge of QD0, a maximum power density of about 4 mW g⁻¹ can be reached inside the NbTi coils. If a 3 mm Tungsten liner (corresponding to about 1 radiation length) is used to thicken the beam pipe and spread out the showers at the location of the loss, the maximum power density can be brought down to about 0.3 mW g⁻¹ in the same conditions. Based on these numbers, we use 1 W as the maximum value for the power deposited on the edge of QD0. This 1 W ↔ 0.3 mW g⁻¹ equivalence, found between total incident power and power density in QD0, will have to be checked for other magnet configurations and beam parameters, especially in the case of the sextupoles.

3. Final doublet optimisation

In this section, we shall discuss our optimisation of the final doublet layout. We shall start with the optimisation of QD0. Several studies of the power deposition into QD0 [4] have shown that the charged beam loss and the loss from radiative Bhabhas exceed the quench limits of the coils, for some of the proposed beam parameters. Therefore, the goal of our optimisation is to reduce these

losses to acceptable levels, for all beam parameters. Note that we work in terms of total incident power, and consider the conversion to localised losses separately (see section 2.5). The optimisation procedure described in the following is applied to all three final doublet designs outlined in section 2.

The underlying principle is, in the first instance, to make the magnet as short as possible within the constraints of the available pole tip field. Hence we begin by increasing the field of QD0 to the maximum possible value, and decrease the length in proportion.

We then perform a scan of the aperture and pole tip field, adjusting the length to maintain the overall focusing strength, and using the total power deposition from the different beam parameter sets as figure of merit. The magnitude of the beamstrahlung energy loss for the Low Power and High Luminosity beam parameters is such that these sets dominate the optimisation. Both the effects from the charged beam, for vertical offsets at the interaction point maximising the beamstrahlung losses, and the combined effects of radiative Bhabhas and the charged beam (collided in this case without a significant vertical offset) are considered. We generally find a minimum in the total power deposition which is very similar for all parameters sets, as the dependence of the total power versus aperture and length found from the scanning is rather shallow. This procedure allows a power-optimised QD0 length, aperture and pole tip field, with the constraints of maintaining the constant integrated focusing strength needed to achieve the required demagnification and keeping the pole tip below a given assumption on the maximum value achievable. Note that the former constraint maintains the demagnification of the final telescope, and also maintains the integrated strength of QF1. To ensure that the minimum we reach in the 3-dimensional space of the scan is a true and global minimum, we begin with a variety of initial magnet conditions (i.e. origin in our space). We find that we always converge to the same point in all cases. We perform this optimisation for the three cases we consider in this work and the result is a set of three QD0-QF1 systems. Note we assume no variation of maximum pole-tip field on magnet aperture.

Once QD0 has been optimised, we can fit for the local chromaticity correction sextupoles. For these sextupoles, located in the immediate vicinity of the final doublet quadrupoles, we assume the same maximum pole tip fields as in the baseline. The chromaticity is corrected, and the required sextupole strengths calculated, by using a simplified model of the system, consisting of the final doublet region and two upstream bends to generate the required dispersion. The bend strengths are fitted to give $\eta_x = 0$ and $\eta'_x = -10\text{mrad}$ at the interaction point. Note that the latter value is chosen to give acceptable sextupole strengths, whilst maintaining the beam angular divergence close to its intrinsic value. While a full treatment of the final focus chromaticity correction includes the condition of zeroing the T_{126} and T_{346} matrix element across the full system, it has been shown that, to a good approximation, sextupole strengths consistent with those in such a full treatment can be obtained by zeroing the T_{166} and T_{346} matrix elements across the simplified system [8]. We apply such a procedure to compute the sextupole strengths in this work. The inter-magnet distances chosen are shown in table 4. In this work, the optics code MAD [9] was used to compute the chromaticity correction.

The length of the optimised sextupoles was chosen to give a reasonable starting point for the beam transport. The sextupole lengths are hence not fully optimised, and require some further study. To optimise the sextupole apertures, a fit is performed, within the maximal value assumed for the pole tip fields, and requiring no loss when transporting a Nominal, Low Power or High

	NbTi, 500 GeV [m]	NbTi, 1 TeV [m]	Nb ₃ Sn, 1 TeV [m]
QD0-SD0	0.8	0.3	0.3
SD0-QF1	5.7	4.9	4.9
QF1-SF1	0.5	0.3	0.3

Table 4. The inter-magnet drift spaces used in the final doublet. In all the layouts, ℓ^* is taken to be 4.5 m, and the total QD-QF distance is always 9 m.

Magnet	Length [m]	Strength	radial aperture [mm]	gradient [T m ⁻¹]	B ^{PT} [T]
QD0	1.23	-0.1940 m ⁻¹	39	161.6	6.30
SD0	2.5	1.1166 m ⁻²	76	-	2.69
QF1	1.0	0.0815 m ⁻¹	15	67.9	1.02
SF1	2.5	-0.2731 m ⁻²	151	-	2.59

Table 5. Quadrupole and sextupole parameters at $\sqrt{s}=500$ GeV for NbTi.

Magnet	Length [m]	Strength	radial aperture [mm]	gradient [T m ⁻¹]	B ^{PT} [T]
QD0	2.47	-0.0970 m ⁻¹	39	161.7	6.31
SD0	3.8	0.5993 m ⁻²	87	-	3.78
QF1	2.0	0.0407 m ⁻¹	15	67.8	1.02
SF1	3.8	-0.1644 m ⁻²	146	-	2.92

Table 6. Quadrupole and sextupole parameters at $\sqrt{s}=1$ TeV for NbTi.

Luminosity beam. The inter-magnet spacings were optimised for beam transport. The technological constraints limit the maximum aperture, and we fit the aperture by requiring no loss when transporting a Nominal, Low Power or High Luminosity beam. The available aperture is computed from the quadratic rise of the field in the beampipe of the sextupole. Note that we consider both the radiative Bhabha contribution to the power deposition and the effect of a vertically offset beam. The requirement of small enough loss (1 W in total) is very stringent, particularly in the case of the High Luminosity offset beams, and results in large sextupole apertures. These could be considerably reduced by relaxing the beam transport requirement, for instance if one would avoid beam parameter optimisations with very large beamstrahlung energy losses.

The results of the optimisation can be found in table 5 for NbTi at 500 GeV, in table 6 for NbTi at 1 TeV and in table 7 for Nb₃Sn at 1 TeV. These tables show the magnet parameters of the two quadrupoles and two sextupoles making up the final doublet layout.

4. Particle losses in the optimised final doublet

In this section, power depositions from particle losses are computed for the three optimised final doublets described in section 2. For completeness we include the power losses for the current baseline layout, both at 500 GeV and 1 TeV. The disrupted beam was calculated using the beam-

Magnet	Length [m]	Strength	radial aperture [mm]	gradient [T m ⁻¹]	B ^{PT} [T]
QD0	2.0	-0.12 m ⁻¹	44	200	8.80
SD0	3.8	0.6454 m ⁻²	95.1	-	4.87
QF1	2.0	0.0407 m ⁻¹	15	67.8	1.02
SF1	3.8	-0.1689 m ⁻²	163	-	3.74

Table 7. Quadrupole and sextupole parameters at $\sqrt{s}=1$ TeV for Nb₃Sn.

beam simulator GUINEA-PIG [10], with the beam parameters taken from [3, 5], and the particle ray-tracing was performed using the programme DIMAD [11]. We find that it is necessary to primarily consider the Low power and High Luminosity beam parameter sets, due to their high beamstrahlung energy loss. We also conservatively consider the transport of the disrupted beam for collisions with vertical offsets chosen to maximise the corresponding beamstrahlung energy loss. Such offsets, typically of about a hundred microns, are expected in the course of tuning the accelerator, in particular during the settling of the trajectory feedback system at the IP. For the normal luminosity-producing zero offset collisions, the effect of radiative Bhabha processes is included. We use 1.28 million macroparticles to represent the disrupted charged beam. The resulting minimum power loss is of order 0.5 to 1 W, which can hence be considered as the upper bound for cases with zero particle loss.² The radiative Bhabha losses, on the other hand, are not statistics limited.

4.1 Results for E=500 GeV

In table 8 we show, for reference, the power losses for the baseline lattice at 500 GeV. This lattice is obtained by scaling down the 1 TeV magnet parameters. Table 9 shows the power losses for the optimised 500 GeV NbTi lattice, produced following the procedure described in section 3 and using the limits for the magnet parameters listed in table 3. Note that the outer pocket radius of QF1 was increased by 1 mm (from 115 mm to 116 mm) to accommodate the charged beam of the high luminosity parameter set with a vertical offset. Comparison of the performance of the baseline final doublet at 500 GeV, table 8, with the performance of the new NbTi doublet optimised for 500 GeV, table 9, shows the benefit of the new final doublet layout. The power losses for all parameter sets are greatly reduced and, following the arguments about quenching of superconducting magnets in section 2, the power losses should be small enough for successful beam transport to be achieved.

Figure 1 illustrates how much the power losses would be further reduced if research and development provided a stronger (i.e. larger) magnetic gradient. This curve shows the power deposition from radiative Bhabhas for the High Luminosity beam parameter set, as a function of magnet scale factor for the optimised NbTi 500 GeV final doublet (solid curve) and the same magnet with an extra 20% of gradient in QD0.

Figure 2 shows the power deposition from radiative Bhabhas for the Low Power beam parameter set, as a function of the QD0 aperture. The minimum in the power loss curve is reasonably shallow, which could be used to reduce the large external size of the magnet. Note that also including the charged beam losses may move this total minimum to slightly larger aperture.

²Strictly speaking the 95% confidence level upper limit is three times this value, or 1.5 to 3 W.

Beam	QD0 [W]	SD0 [W]	QF1 [W]	SF1 [W]
Nominal	0	0	0	0
Nominal (dy=200nm)	0	0	0	0
Nomial RB	0.40	0	0.01	0.11
low power	7.61	0	0	469.76
Low power (dy=120nm)	7.77	0	0	188.05
Low power RB	0.39	0	0.01	0.10
High lum.	91.81	0	0	1399.82
High lum. (dy=120nm)	88.86	0	5.42	192.52
High lum. RB	0.97	0	0.03	0.25

Table 8. The power losses on the magnets for the baseline NbTi 500 GeV lattice.

Beam	QD0 [W]	SD0 [W]	QF1 [W]	SF1 [W]
Nominal	0	0	0	0
Nominal (dy=200nm)	0	0	0	0
Nomial RB	0.05	0	0.13	0.03
low power	0	0	0	0
Low power (dy=120nm)	0	0	0	0
Low power RB	0.05	0	0.13	0.03
High lum.	0	0	0	0
High lum. (dy=120nm)	0	0	0	0
High lum. RB	0.12	0	0.33	0.08

Table 9. The power losses on the magnets for the optimised NbTi 500 GeV lattice.

Finally, the linear optics for the baseline final doublet and the optimised NbTi final doublet at 500 GeV (nominal parameters) can be seen in figures 3 and 4.

4.2 Results for E=1 TeV

In table 10 we show, for reference, the power losses for the baseline lattice at 1 TeV. Table 11 shows the power losses in the NbTi final doublet, optimised for 1 TeV. The low maximum gradient possible with this magnet technology means that, whilst the losses are lower than the baseline design at 1 TeV, they are still too high to avoid magnet quenching. This indicates that higher gradient magnets are required.

Finally, table 12 shows the power losses in the Nb₃Sn final doublet, optimised for 1 TeV. The higher gradients expected from using Nb₃Sn superconductive material enable to significantly reduce the power deposition as compared to both the baseline and optimised NbTi final doublet designs. However, the losses are still in excess of the quenching limits of the magnets. To understand what improvement in superconducting technology would be required, we computed how much larger the pole tip field in QD0 would need to be to bring the sum of the charged beam and radiative Bhabha losses to less than 1W, for the Low Power beam parameter set. The result was

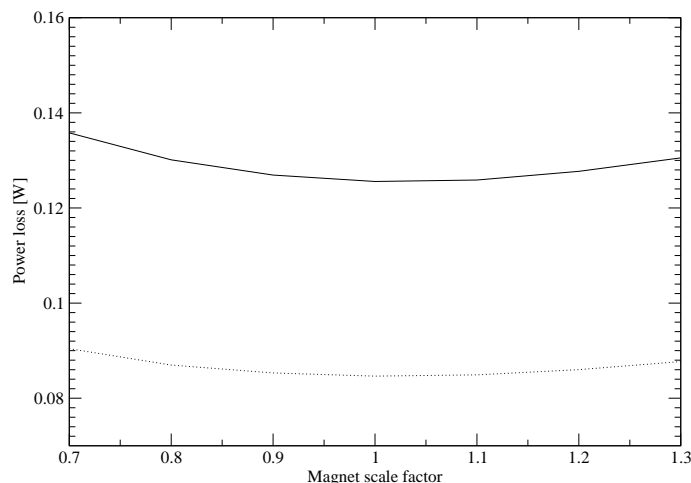


Figure 1. The beneficial effect of a 20% gradient increase, for the High Luminosity parameter set radiative Bhabha losses. The solid line is the power losses for the NbTi 500 GeV optimised doublet described in the text, and the dotted line shows the power losses achieved if an extra 20% of magnetic gradient became available.

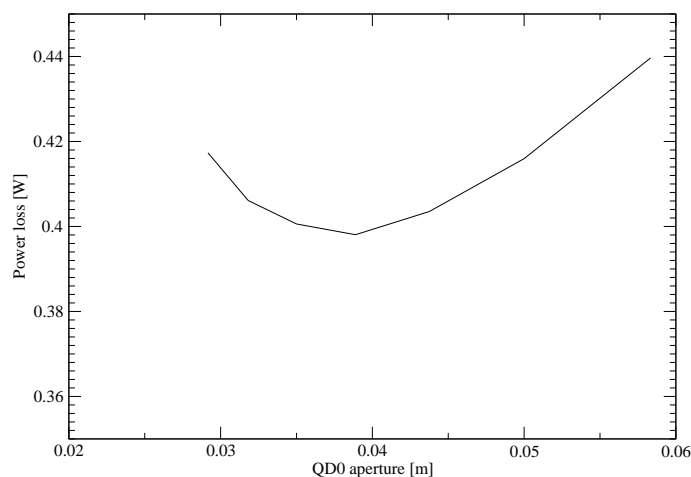


Figure 2. The power loss from the Low Power parameter set radiative Bhabhas, as a function of the QD0 aperture. This plot shows the shallow minimum in the power loss curve, which could be used to reduce the large external size of the magnet. Note, the dependence shown here is for the baseline doublet at 500 GeV. A similarly shallow behaviour is obtained for the other cases.

that a pole tip field of 11T in a magnet with an aperture of 35 mm would be needed for the Low Power beam parameter set to be accommodated in the final doublet at 1 TeV. The feasibility of such large pole tip fields on the time-scale of the 1 TeV energy upgrade of the ILC needs to be discussed with relevant superconductive magnet experts. Alternatively, beam parameters at 1 TeV may be optimised with somewhat lower beamstrahlung energy loss, including for total beam powers as low as in the present Low Power parameter set. Such sets would result in significantly easier final doublet designs.

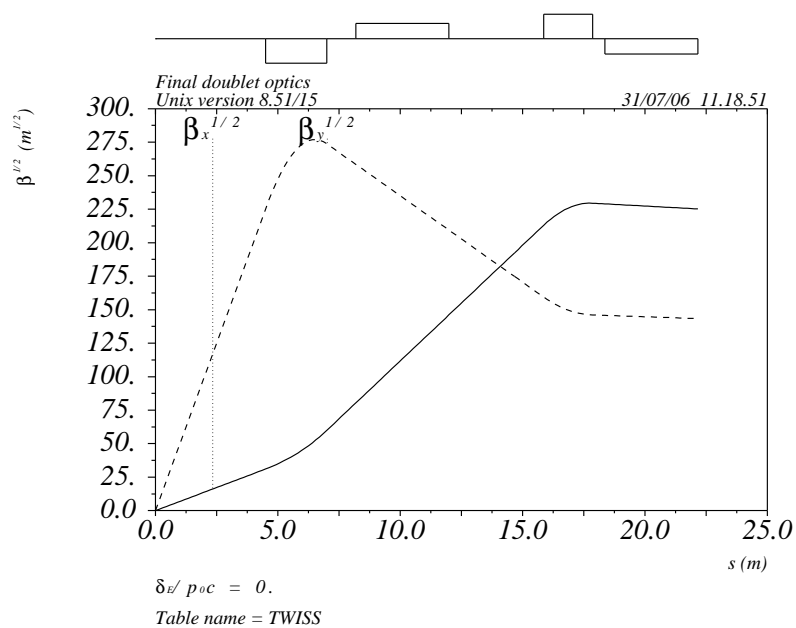


Figure 3. The linear optics in the baseline final doublet for the nominal parameters at 500 GeV.

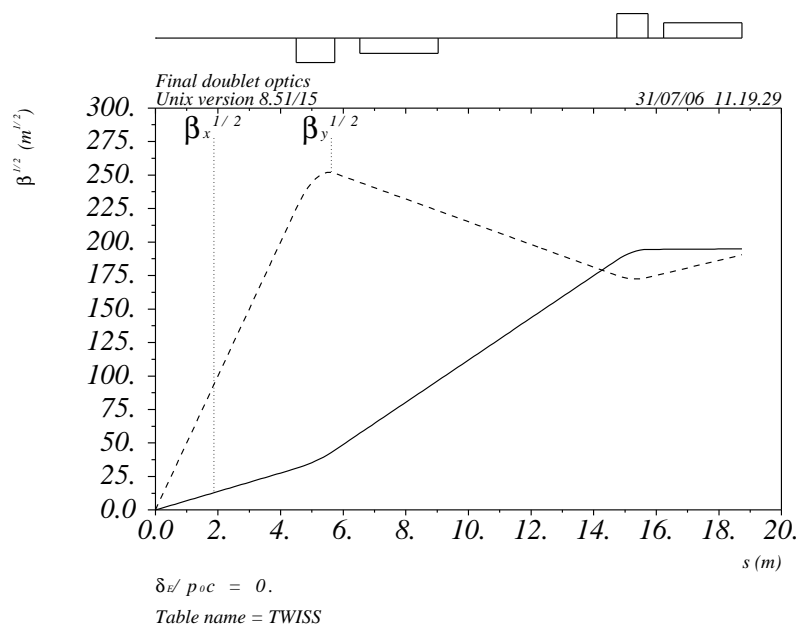


Figure 4. The linear optics in the optimised NbTi final doublet for the nominal parameters at 500 GeV.

5. Conclusions

In this note, we have described a detailed study of the power deposition in the final doublet of the ILC 2 mrad crossing-angle layout, from both the disrupted charged beam and from the radiative

Beam	QD0 [W]	SD0 [W]	QF1 [W]	SF1 [W]
Nominal	0	0	0	0
Nominal (dy=100nm)	3.39	0	0	0
Nominal RB	1.02	0	0.01	0.30
Low Power	755.05	0	7.63	95.37
Low Power (dy=120nm)	897.46	0	20.98	109.49
Low Power RB	1.19	0	0.03	0.34
High Lum.	8430.59	0	190.17	878.12
High Lum. (dy=80nm)	14076.00	0	454.53	1514.45
High Lum. RB	3.60	0	0.11	0.92

Table 10. The power losses on the magnets for the baseline 1 TeV lattice.

Beam	QD0 [W]	SD0 [W]	QF1 [W]	SF1 [W]
Nominal	0	0	0	0
Nominal (dy=100nm)	0	0	0	0
Nominal RB	0.73	0	0.06	0.16
Low Power	223.94	27.85	5.76	8.07
Low Power (dy=120nm)	271.85	6.77	11.39	10.66
Low Power RB	0.15	0	0.39	0.10
High Lum.	3169.79	703.78	54.96	122.87
High Lum. (dy=80nm)	5501.98	409.85	352.71	236.43
High Lum. RB	2.55	0	0.12	0.36

Table 11. The power losses on the magnets for the NbTi 1 TeV lattice.

Beam	QD0 [W]	SD0 [W]	QF1 [W]	SF1 [W]
Nominal	0	0	0	0
Nominal (dy=100nm)	0	0	0	0
Nominal RB	0.32	0	0.34	0.10
Low Power	20.52	0	28.73	27.56
Low Power (dy=120nm)	7.77	0	48.03	40.71
Low Power RB	0.37	0	0.39	0.12
High Lum.	264.42	0	477.77	439.98
High Lum. (dy=80nm)	473.00	0	1286.15	670.40
High Lum. RB	1.09	0	1.19	0.36

Table 12. The power losses on the magnets for the Nb₃Sn 1 TeV lattice.

Bhabha events. We exploited superconductive magnet technologies both currently available and expected to be developed through on-going R&D: NbTi and Nb₃Sn with maximum pole tip fields of respectively 6.28 T and 8.8 T.

We find that using NbTi technology to optimise the 500 GeV baseline final doublet is adequate to obtain small enough beam power depositions in the final doublet, provided a Tungsten liner is included in the design of the vacuum chamber to spread out the showers and reduce the maximum power density at the location where most losses are concentrated. This doublet now needs to be integrated into the final focus system and extraction line. When this will be done, we will propose that it become the baseline for the 2 mrad at 500 GeV, with the assumption that it would have to be replaced at the time of the 1 TeV energy upgrade. In all cases, the sextupole lengths, strengths and apertures are not fully optimised. Some more work is still needed here, in view of reducing their sizes and ease their integration with the detector. It is also necessary to include the extraction line magnets in a further optimisation.

A final doublet based on NbTi technology does not, on the other hand, provide small enough beam power depositions at 1 TeV, for several of the beam parameter sets considered. Exploiting Nb₃Sn superconductive technology can however improve the situation considerably, as the higher expected gradients would allow significantly lower power depositions. The optimised layout shows far superior power loss behavior than the current 1 TeV machine baseline final doublet, but is still in excess of the quenching limit for the beam parameter sets with the largest beamstrahlung energy loss. A 35 mm QD0 with a pole tip field of around 11 T would be needed to avoid quenching of this magnet, in the case of the Low Power beam parameters.

We expect further R&D in superconductive magnet technology to enable increases in maximum available pole tip field in the future, which will ease the design of the 2 mrad beam crossing-angle layout. An alternative path is to constrain the optimisation of the beam parameters at 1 TeV with an upper bound on the beamstrahlung energy loss. This would also be motivated since a very large beamstrahlung energy loss is undesirable for several other reasons.

Acknowledgments

We would like to thank Andrei Seryi and Deepa Angal-Kalinin for helpful advice and assistance, Brett Parker for clarifying the effect of an external solenoid field on the maximum field of superconductive magnets, Lew Keller and Takashi Maruyama for discussions on localised power density calculations, Grahame Blair for useful advice and John Carter for his assistance computing the effect of a Tungsten liner in the vacuum chamber.

References

- [1] The ILC BCD, http://www.linearcollider.org/wiki/doku.php?id=bcd:bcd_home
- [2] The NLC Design Group, *Zeroth order design report for the Next Linear Collider*, SLAC-R-0474
- [3] D. Schulte, *Beam-beam simulations of the proposed ILC parameters*, EuroTeV memo 2005-004-1 (2005).
- [4] Y. Nosochkov et al. , *Optics of the ILC extraction line for 2 mrad crossing angle*, EuroTeV report 2006-001-01 (2006).
- [5] ILC Global Design Effort, *Parameters for the linear collider* (2003) http://www.fnal.gov/directorate/icfa/LC_parameters.pdf

- [6] Bruning et. al. , LHC project report 785, *Performance limits and IR design of a possible LHC luminosity upgrade based on NbTi SC magnet technology*, CARE-Conf-04-005-HHH.
- [7] R. Appleby, the proceedings of LCWS06, India, 9-13 March 2006.
- [8] A. Seryi, *Unit 6 of Physics and Technology of Linear Collider Facilities*, US-PAS, Santa Barbara, June 2003.
- [9] F. Christoph Iselin, *The MAd program reference manual*, CERN, LEP Division 1, 1984.
- [10] D. Schulte, PhD thesis, *Study of electromagnetic and hadronic background in the interaction region of the TESLA Collider*, The University of Hamburg, TESLA-97-08 (1996).
- [11] R. Servranckx et. al. , DIMAD manual.